Pergamon

PII: S0965-1748(96)00083-5

Insect Biochem. Molec. Biol. Vol. 27, No. 2, pp. 101–108, 1997
Published by Elsevier Science Ltd

0965-1748/97 $17.00 + 0.00

Rapid Communication

Catecholamine and Histidyl Protein Cross-Linked Structures in Sclerotized Insect Cuticle

RONGDA XU,† XIN HUANG,‡ THEODORE L. HOPKINS,† KARL J. KRAMER*§

(Received 20 September 1996; revised and accepted 15 October 1996)

Catecholamines play an important role in cuticular sclerotization, an extracellular process used by insects at various stages of their life cycle to stabilize their exoskeletons. Analysis of products derived from the acid hydrolysis of insect cuticle provide for the first time direct structural evidence for the actual cross-links between catecholamines and histidyl residues of the cuticular proteins. Four adducts were purified by HPLC from a 6 M HCl hydrolysate of tobacco hornworm, *Manduca sexta*, sclerotized pupal cuticle. They were identified as 7-N^{τ}-, 6-N^{τ}-, 7-N^{π}-, and 6-N^{π}-histidyldopamine adducts using matrix-assisted laser desorption ionization mass spectrometry, 1D ^{1}H NMR, and 2D homonuclear nuclear Overhauser effect NMR spectroscopy in combination with molecular modeling. The molar ratio of these adducts in the hydrolysate was approximately 6:3:2:1, respectively. These adducts apparently are formed from Michael 1,4- and 1,6-addition reactions of the putative quinonoid sclerotizing agents, *N*-β-alanyldopamine quinone and *N*-β-alanyldopamine quinone methide, with both imidazole nitrogens of histidyl residues of proteins. Published by Elsevier Science Ltd

Catecholamine Quinone Oxidation Addition Adduct Histidine Protein Cross-Links Insect Cuticle Sclerotization

INTRODUCTION

Sclerotization or tanning is a complex process in animals in which proteinaceous structures are stabilized by reactions with quinones to yield greater strength and rigidity (Pryor, 1962; Waite, 1990). It is utilized extensively by insects at various stages of their life cycles to stiffen and harden exoskeletons, egg shells, egg cases, and various silk structures (Sugumaran, 1988; Hopkins and Kramer, 1992; Andersen *et al.*, 1996). However, because of the resistance of sclerotized proteins to chemical and physical degradation, very little direct evidence for their structures has been obtained since Pryor more than 50 years ago proposed a chemical model that involves cross-linking by quinone tanning (Pryor, 1940).

Based on reactions of model compounds, solid-state NMR spectroscopy of sclerotized structures, and cuticular protein chemistry, it is now accepted widely that post-translational modifications that lead to cross-links between cuticular proteins and catecholamines play a crucial role in sclerotization (Schaefer *et al.*, 1987; Sugumaran, 1988; Andersen *et al.*, 1991, 1992, 1996; Christensen *et al.*, 1991; Hopkins and Kramer, 1992; Okot-Kotber *et al.*, 1994, 1996; Kramer *et al.*, 1995). This process apparently involves the oxidation of two catecholamines, *N*-acetyldopamine (NADA) and *N*-β-alanyldopamine (NBAD), to quinonoid sclerotizing agents followed by nucleophilic addition reactions with certain functional groups of cuticular proteins (Sugumaran, 1988; Hopkins and Kramer, 1992; Andersen *et al.*, 1996). When radiolabeled histidine, lysine, or tyrosine were injected into dipteran larvae and incorporated into cuticle, uncharacterized radiolabeled products from puparial hydrolysates of the sclerotized cuticle were detected, which indicated that these amino acids and/or their metabolites are involved in cross-link formation during

*Author for correspondence. Tel.: (913) 776-2711; Fax: (913) 537-5584; E-mail: kramer@usgmrl.ksu.edu

†Department of Entomology Kansas State University, Manhattan, KS 66506, U.S.A.

‡Department of Chemistry, Kansas State University, Manhattan, KS 66506, U.S.A.

§Grain Marketing and Production Research Center, Agricultural Research Service, United States Department of Agriculture, Manhattan, KS 66502, U.S.A.

sclerotization (Sugumaran and Lipke, 1982). More recently, solid-state NMR experiments have provided the strongest evidence to date for the presence of protein–catecholamine cross-links in insect cuticle (Schaefer *et al.*, 1987; Christensen *et al.*, 1991; Kramer *et al.*, 1995). These NMR analyses detected covalent bonding between either the aromatic ring carbons or the β-carbon (C7) of the dopamine side chain and histidyl residues of the cuticular proteins (Schaefer *et al.*, 1987; Christensen *et al.*, 1991; Kramer *et al.*, 1995). In addition, proteins covalently bonded to catecholamines have been isolated from cuticle undergoing sclerotization (Okot-Kotber *et al.*, 1994, 1996). Model reactions of catecholamine quinones with amino acid derivatives representing nucleophiles in cuticular proteins have been studied to determine potential candidate structures of the natural adducts (Andersen *et al.*, 1991, 1992; Xu *et al.*, 1996). Coupling between NADA and *N*-acetylhistidine was catalyzed *in vitro* by cuticular enzyme preparations, and both side chain C7- and ring C6-addition products were identified (Andersen *et al.*, 1991, 1992). Model compound reactions between electrochemically prepared NADA quinone and *N*-acetylhistidine produced ring C6- and C2-adducts (Xu *et al.*, 1996).

Although the presence of covalent bonding between proteins and catecholamines in insect cuticle has been established and model studies have shown that catecholamine quinones do form adducts at several sites with amino acids, the actual structures of the protein–catecholamine adducts have not been elucidated. To determine the stable catecholamine–amino acid cross-link structures formed during the sclerotization of insect cuticular proteins, we first hydrolysed *Manduca sexta* pupal exuvial cuticle in 6 M HCl and then isolated and characterized four histidyldopamine adducts (His–DA) from a complex mixture of hydrolysis products.

MATERIALS AND METHODS

Air-dried *M. sexta* pupal exuvial cuticle was ground in dry ice and lyophilized. In a 20 ml vacuum hydrolysis tube, 0.25 g cuticle was mixed with 5 ml 6 M HCl containing 5% phenol and heated at 110°C for 24 h *in vacuo*. To selectively recover the products containing catechols, the supernatant from the hydrolysate was subjected to alumina adsorption using a procedure similar to that previously reported (Hopkins *et al.*, 1984). The hydrolysate was adjusted to pH 8.9 with a saturated Trizma base solution. EDTA (1 g) and alumina (2 g) were added to the solution and stirred for 15 min. The mixture was centrifuged, and the supernatant was subjected to alumina (2 g) adsorption again. The alumina solids were pooled and washed with distilled water, and then the catechols were desorbed twice in 2 ml 1 M HOAc for 15 min. The HOAc solutions were pooled and used for HPLC analysis and isolation of catechol-containing products.

The HPLC system consisted of a Hewlett-Packard 1050 Series HPLC quaternary pump, on-line degasser, and diode array detector (DAD), and was controlled by a HPLC^{3D} ChemStation. The eluants were monitored at 280 nm, which is near the λ_{max} of most catecholamines and their amino acid adducts. A binary mobile phase consisted of solvent A, 0.15 M formic acid and 0.03 M ammonium formate (pH 3.0), and solvent B, a 1:1 mixture of methanol and a solution of 0.3 M formic acid and 0.06 M ammonium formate. Phenomenex Spherisorb 5 ODS-2 (5 μm, 250×21.2 mm) and Phenomenex Prodigy ODS2-PREP (10 μm, 250×10 mm) columns were used. For the Spherisorb column, the flow rate was 4 ml/min, and the mobile phase gradient was 0–10 min, 0% solvent B, and 10–40 min, linear gradient from 0% solvent B to 100% solvent B. For the Prodigy column, the flow rate was 2 ml/min and the mobile phase gradient was 0–5 min, 0% solvent B, and 5–20 min, linear gradient from 0% to 100% solvent B. Matrix-assisted laser desorption ionization–mass spectrometry (MALDI–MS) was performed on a Finnigan Lasermat 2000 mass spectrometer using α-cyano-4-hydroxycinnamic acid as the matrix. The following NMR experiments were carried out either with a Varian UNITY*plus* 400 MHz spectrometer at 27°C or with a Varian UNITY*plus* 500 MHz spectrometer at 30°C: proton, heteronuclear multiple-bond correlation (HMBC), and homonuclear nuclear Overhauser effect spectroscopy (NOESY). Products were dissolved in 0.7 ml of either D_2O or H_2O:D_2O (90:10).

Molecular modeling was performed to assist in the interpretation of the NOE connectivities on a Silicon Graphics workstation using QUANTA/CHARMm software. Grid scan conformational searching was performed on two dihedral angles in the structures, whereas the other dihedral angles were adjusted to give the lowest potential energy at each searching step. The contour plots of potential energy change as a function of the dihedral angle were evaluated and the conformations with lowest potential energy were used to interpret the NOESY spectra, in which the interatomic distance (r) plays an important role and the proton connectivities through space are revealed by off-diagonal cross-peaks. NOE intensities were determined based on the ratios of the volume integrals of cross-peaks and H2′ diagonal-peaks (see Fig. 4 for atomic numbering).

RESULTS AND DISCUSSION

Catechols were recovered using alumina adsorption after the *M. sexta* pupal exuvial cuticle was hydrolysed in 6 M HCl for 24 h. These catechols were separated by reversed-phase HPLC using the Spherisorb column (Fig. 1A). This step yielded homogeneous compounds I and II and a fraction containing a mixture of compounds III and IV plus other catechol containing products. The mixture containing III and IV was lyophilized, and the constituents were purified to homogeneity by chromatography on the Prodigy column (Fig. 1B). MALDI–MS analysis showed that compounds I to IV all had the same

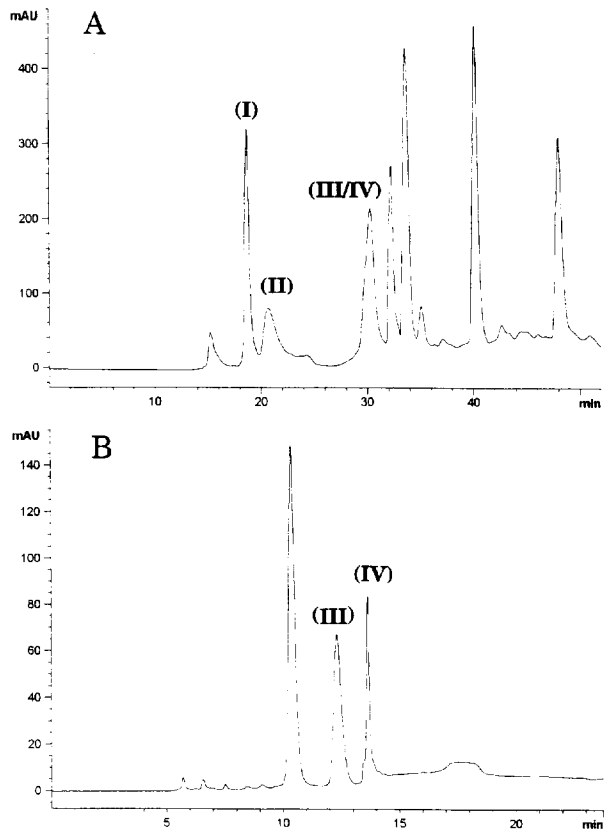

FIGURE 1. Semipreparative chromatographic separation of catechol-containing compounds in *M. sexta* pupal exuvial cuticle hydrolysate. (A) LC–UV (280 nm) of hydrolysate using Phenomenex Spherisorb 5 ODS-2 (250×21.20 mm) column; (B) LC–UV (280 nm) of fraction III/IV from (A) using Phenomenex Prodigy 10 m ODS-2 (250×10 mm) column.

molecular mass of 306 Da, consistent with that of histidyldopamine adducts (His–DA).

^{1}H NMR analysis revealed the identities of compounds I and III as C7- (or β-) adducts, which had absorption maxima at 280 nm, and compounds II and IV as C6-adducts, which had absorption maxima at 284 nm. The ^{1}H NMR (400 MHz) assignments of the four purified histidyldopamine adducts are as follows (the final assignments of the structures required not only 1D NMR data, but also NOESY and molecular modeling data as described below):

7-N^{τ}-His–DA (I): δ=7.86 (s, 1H, H2′), 7.20 (s, 1H, H5′), 6.94 (d, 1H, J=8 Hz, H5), 6.90 (d, 1H, J=2 Hz, H2), 6.88 (dd, 1H, J=8 Hz, J=2 Hz, H6), 5.54 (dd, 1H, J=9 Hz, J=6 Hz, H7), 3.96 (t, 1H, J=6 Hz, H7′), 3.85 (dd, 1H, J=13 Hz, J=9 Hz, H8a), 3.75 (dd, 1H, J=13 Hz, J=6 Hz, H8b), 3.10 (d, 2H, J=6 Hz, H6′);

6-N^{τ}-His–DA (II): δ=8.05 (s, 1H, H2′), 7.24 (s, 1H, H5′), 6.94 (s, 1H, H5), 6.96 (s, 1H, H2), 4.04 (t, 1H, J=6 Hz, H7′), 3.28 (dd, 1H, J=15 Hz, J=6 Hz, H6′a), 3.20 (dd, 1H, J=15 Hz, J=6 Hz, H6′b), 2.98 (t, 2H, J=8 Hz, H8), 2.66 (dd, 2H, J=13 Hz, J=8 Hz, H7);

7-N^{π}-His–DA (III): δ=7.94 (s, 1H, H2′), 7.20 (s, 1H, H5′), 6.92 (d, 1H, J=8 Hz, H5), 6.86 (d, 1H, J=2 Hz, H2), 6.80 (dd, 1H, J=8 Hz, J=2 Hz, H6), 5.38 (dd, 1H, J=8 Hz, J=5 Hz, H7), 4.18 (dd, 1H, J=12 Hz, J=8 Hz, H8a), 4.12 (dd, 1H, J=12 Hz, J=5 Hz, H8b), 3.90 (t, 1H, J=6 Hz, H7′), 3.18 (dd, 1H, J=16 Hz, J=6 Hz, H6′a), 3.08 (dd, 1H, J=16 Hz, J=6 Hz, H6′b);

6-N^{π}-His–DA (IV): δ=7.82 (s, 1H, H2′), 7.23 (s, 1H, H5′), 7.12 (s, 1H, H5), 7.04 (s, 1H, H2), 4.02 (dd, 1H, J=7 Hz, J=5 Hz, H7′), 3.56 (t, 2H, J=6 Hz, H8), 3.21 (dd, 1H, J=10 Hz, J=5 Hz, H6′a), 3.14 (dd, 1H, J=10 Hz, J=7 Hz, H6′b), 2.55 (t, 2H, J=6 Hz, H7).

The molar ratio of these His–DA adducts, I, II, III, and IV, released in the hydrolysate was estimated from their peak areas in the chromatograms (assuming comparable molar absorption coefficients) to be 6:3:2:1, respectively.

In addition to His–DA adducts, we also have resolved other as yet unidentified catechol-containing hydrolytic products that may represent additional cross-link structures. Several other products were purified from the Spherisorb column (Fig. 1A). The compound eluting at 33.6 min had an absorption maximum at 280 nm and was identified as dopamine by NMR and UV/vis spectroscopy as well as MALDI–MS. The compound eluting at 40.1 min had an absorption maximum at 280 nm. It also was found to be a major product when norepinephrine (NE) was subjected to the conditions of acid hydrolysis in the presence of phenol. NMR data showed that it is an adduct of NE and phenol, 6-phenol-norepinephrine (data not shown). Hence, this adduct is an artifact from the nucleophilic addition of phenol to NE quinone, which was produced from the oxidation of NE released from the cuticle during hydrolysis (Okot-Kotber *et al.*, 1994). The compound eluting at 48.0 min was identified as catechol because it had the same absorption maximum (276 nm) and retention time as a catechol standard. The compound eluting at 32.2 min had an absorption maximum at 280 nm, but its structure is not identified. Another compound obtained from the Prodigy column at 10.4 min coeluted with and had the same absorption maxima (280 and 310 nm) as an arterenone (3,4-dihydroxyphenylketoethanolamine) standard. This ketocatechol-type of compound is present in acid hydrolysates presumably as a degradation product derived from an unknown catecholamine species modified at C7 in the cuticle (Andersen *et al.*, 1996). A control experiment showed that no His–DA adducts or other products mentioned above were produced by heating DA in the presence of a large excess of *N*-acetylhistidine in 6 M HCl containing 5% phenol (data not shown). Therefore, the His–DA adducts obtained from the cuticle hydrolysate were released from cuticle and were not artifacts from hydrolysis.

The His–DA adducts I–IV contain either the 1,4-disubstituted imidazole moiety (N^{τ}-adducts) or the 1,5-disubstituted imidazole moiety (N^{π}-adducts). A previous report noted that use of ^{1}H NMR analysis in aprotic solvents such as dimethylsulfoxide (DMSO) at elevated temperatures could differentiate between some 1,4- and 1,5-disubstituted imidazoles based on small differences

in coupling constants (~0.2 Hz) between their imidazole ring protons (Matthews and Rapoport, 1973). However, the low solubility of the His–DA adducts in DMSO did not allow us to perform such an experiment. To differentiate among the N^{τ}/N^{π} isomers, we first used ^{13}C–^{1}H heteronuclear multiple-bond correlation (HMBC) NMR analysis. However, sufficient spectral data could not be obtained to establish unequivocally the connectivities between the protons on the imidazole ring and the DA carbon that is bonded to the imidazole nitrogen. As an alternative method, we used 2D ^{1}H–^{1}H homonuclear nuclear Overhauser effect NMR spectroscopy (NOESY) to establish the proton connectivities through space (Fig. 2). The mixing times in the NOESY experiments were 400 and 200 ms for the 7-adducts (I and III) and the 6-adducts (II and IV), respectively.

To assist in the interpretation of the NOE connectivities, we performed molecular modeling of the four adducts to determine their preferred conformations. Dihedral angles C2–C1–C7–C8 (angle A) and C1–C7–N1′–C2′ (angle B) were selected for use in the conformational searching for the two 7-adducts (see Fig. 4 for numbering). The conformation of lowest potential energy for 7-N^{τ}-His–DA (Fig. 3I) is the one with dihedral angles A and B (Fig. 4I) of 15° and −50°, respectively, whereas that for 7-N^{π}-His–DA (Fig. 3III) is the one with angles A and B (Fig. 4III) of −35° and −55°, respectively. The conformation of 7-N^{π}-His–DA exhibits an electrostatic

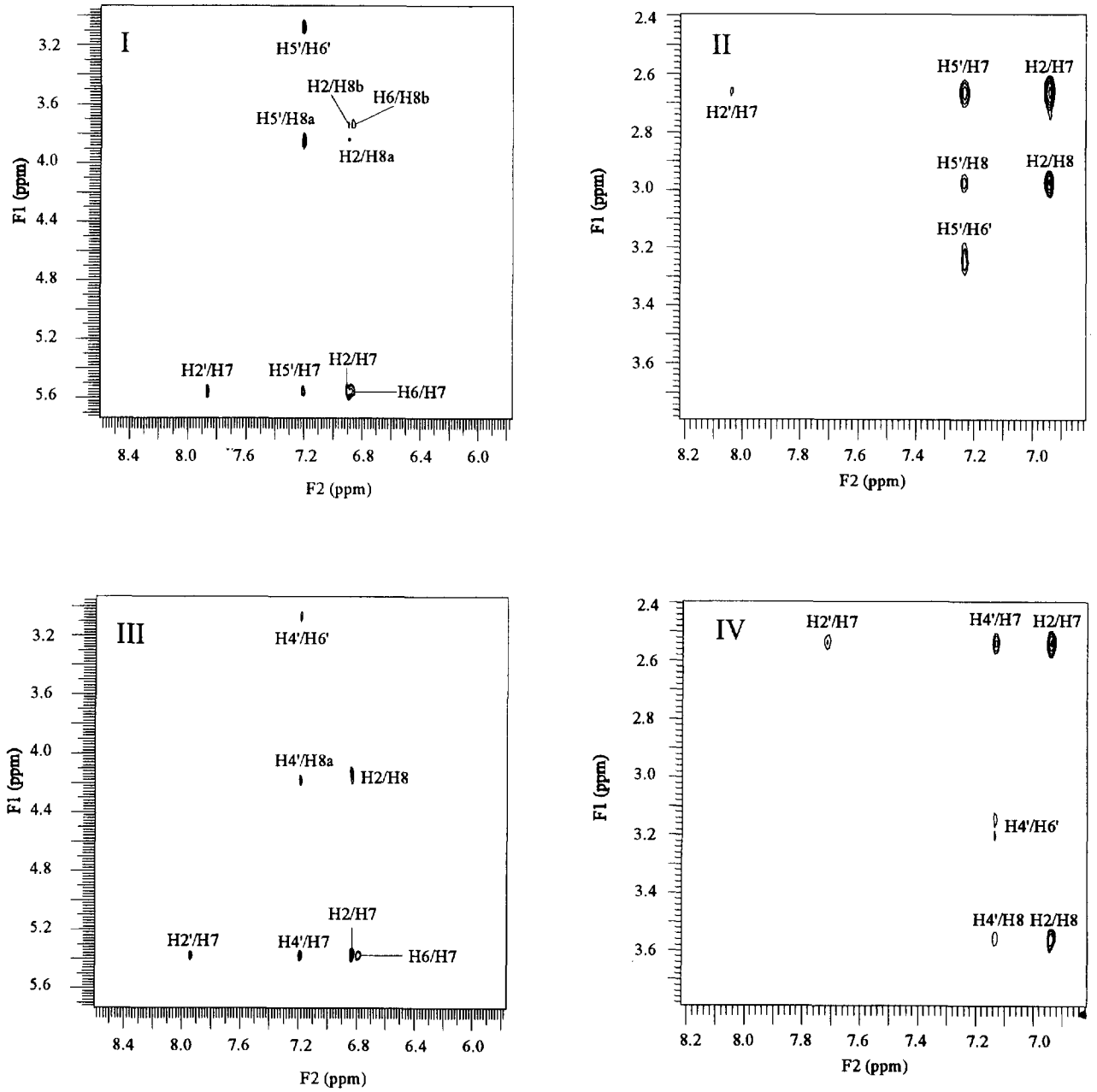

FIGURE 2. Contour plots showing off-diagonal portion of NOE cross-peaks between aromatic protons and aliphatic protons in ^{1}H–^{1}H NOESY NMR spectra of His–DA adducts purified from *M. sexta* pupal exuvial cuticle hydrolysate: 7-N^{τ}-His–DA (I), 6-N^{τ}-His–DA (II), 7-N^{π}-His–DA (III), and 6-N^{π}-His–DA (IV).

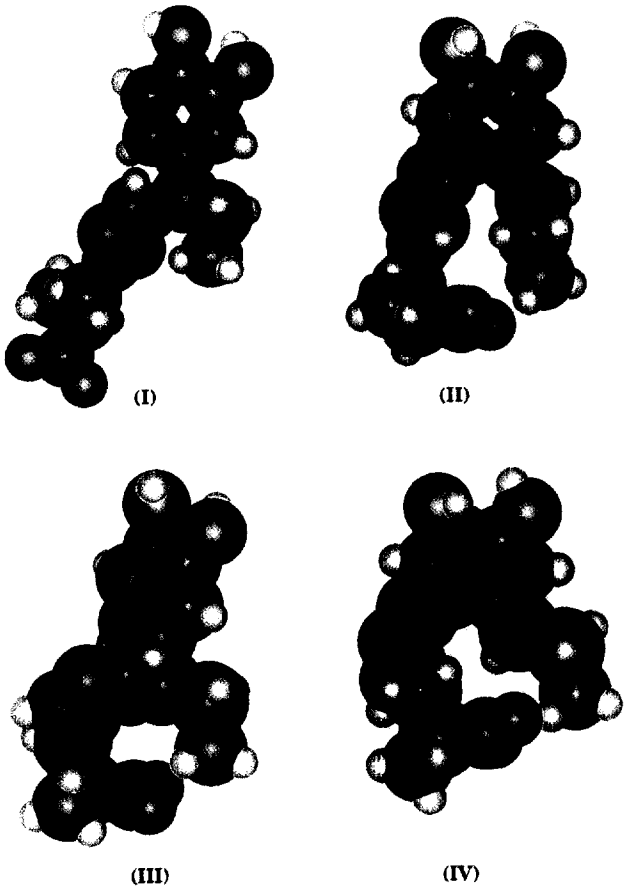

FIGURE 3. Energy-minimized 3D molecular models of isomeric His–DA adducts obtained from insect cuticle hydrolysate: 7-N^{τ}-His–DA (I), 6-N^{τ}-His–DA (II), 7-N^{π}-His–DA (III), and 6-N^{π}-His–DA (IV). Note the electrostatic interaction between the DA amino group and the His carboxyl group in (II), (III), and (IV), but not in (I).

interaction between the DA amino group and the His carboxyl group. However, the conformation of 7-N^{τ}-His–DA does not have such an interaction, because the steric strain would increase substantially if an electrostatic interaction between the His side chain and the DA side chain occurred. Although 7-N^{τ}-His–DA does not exhibit an electrostatic interaction, its potential energy contour plot reveals that low energy conformations fall in a relatively small dihedral angle window, $-30°$ to $30°$ for angle A and $-40°$ to $-60°$ for angle B, so that the rotations of both the DA side chain and the histidyl residue are very limited. On the other hand, although the relative spatial positions of the DA side chain and the His residue in the 7-N^{π}-His–DA are fixed by the electrostatic interaction, the change of angle A from $-180°$ to $180°$ results in only a very small potential energy change when angle B is fixed at $-55°$. This result demonstrates that the DA side chain and the His residue of 7-N^{π}-His–DA can rotate quite freely around the C1–C7 bond. The most distinguishing feature between the two 7-adducts is the position of the protons that are next to the side chain of the histidyl group, i.e. H5′ in 7-N^{τ}-His–DA and H4′ in 7-N^{π}-His–DA. The former proton is relatively close in space to the H7 proton (r =3.8 Å) and at least one of the H8 protons (r=4.4 Å). However, the H4′ in 7-N^{π}-His–DA is oriented far away from the DA side chain by an electrostatic interaction between the DA amino group and the His carboxyl group. The interatomic distance between H4′ and H7 is 4.9 Å and that between H4′ and either of the H8 protons is at least 5.9 Å. These modeling results are consistent with the observation of relatively strong NOE cross peaks for H5′/H7 and H5′/H8 in Fig. 2I and weak NOE cross peaks for H4′/H7 and H4′/H8 in Fig. 2III. Although the areas of H5′/H7 in Fig. 2I and H4′/H7 in Fig. 2III appear similar, the volume integral of the former is greater than that of the latter. Compounds I and III thus were identified as 7-N^{τ}-His–DA and 7-N^{π}-His–DA, respectively (Figs 3 and 4).

Dihedral angles C2–C1–C7–C8 (angle C) and C1–C6–N1′–C2′ (angle D) were selected for use in the conformational searching for the two 6-adducts. The conformation of lowest potential energy for 6-N^{τ}-His–DA (Fig. 3II) is the one with dihedral angles C2–C1–C7–C8 (angle C) and C1–C6–N1′–C2′ (angle D) (Fig. 4II) of 85° and $-115°$, respectively, whereas that for 6-N^{π}-His–DA (Fig. 3IV) is the one with angles C and D of 100° and $-95°$ (Fig. 4IV), respectively. Both of these conformations have the DA amino group and the His carboxyl group juxtaposed toward one another by electrostatic forces, which severely restricts the rotations of both the DA side chain and the histidyl moiety. Similar to the case of the 7-adducts, the most distinguishing feature of the two C6 adducts is the position of the protons that are adjacent to the side chain of the histidyl group, i.e., H5′ in 6-N^{τ}-His–DA and H4′ in 6-N^{π}-His–DA. The former proton is close in space to at least one of the H7 protons (r=3.0 Å) and one of the H8 protons (r=2.1 Å). However, the H4′ proton in 6-N^{π}-His–DA is oriented rather far away from the DA side chain by the electrostatic interaction between the DA amino group and the His carboxyl group. The interatomic distances between H4′ and H7 or H8 are at least 4.7 Å. These modeling results are consistent with the observation of strong NOE cross peaks for H5′/H7 and H5′/H8 in Fig. 2II and weak NOE cross peaks for H4′/H7 and H4′/H8 in Fig. 2IV. Compounds II and IV thus were identified as 6-N^{τ}-His–DA and 6-N^{π}-His–DA, respectively (Figs 3 and 4).

Our results show that sclerotization involves not only the phenyl ring C6 but also the side chain C7 of the catecholamines, as well as both of the imidazole nitrogens (N^{τ} and N^{π}) of histidyl residues in cuticular proteins of the pupal cuticle of *M. sexta*. The identification of electrophilic sites at phenyl ring carbon C6 and side chain carbon C7 of the catecholamines is consistent with a model enzymatic reaction study (Andersen *et al.*, 1991, 1992) and in part with a model chemical reaction study (Xu *et al.*, 1996). However, a ring C2 adduct also was identified in the latter study, which so far has not been detected in the *M. sexta* cuticle hydrolysate. Furthermore, although N^{π}-adducts were not found in the model studies (Andersen *et al.*, 1991, 1992; Xu *et al.*, 1996), they were isolated in substantial amounts from the cuticular

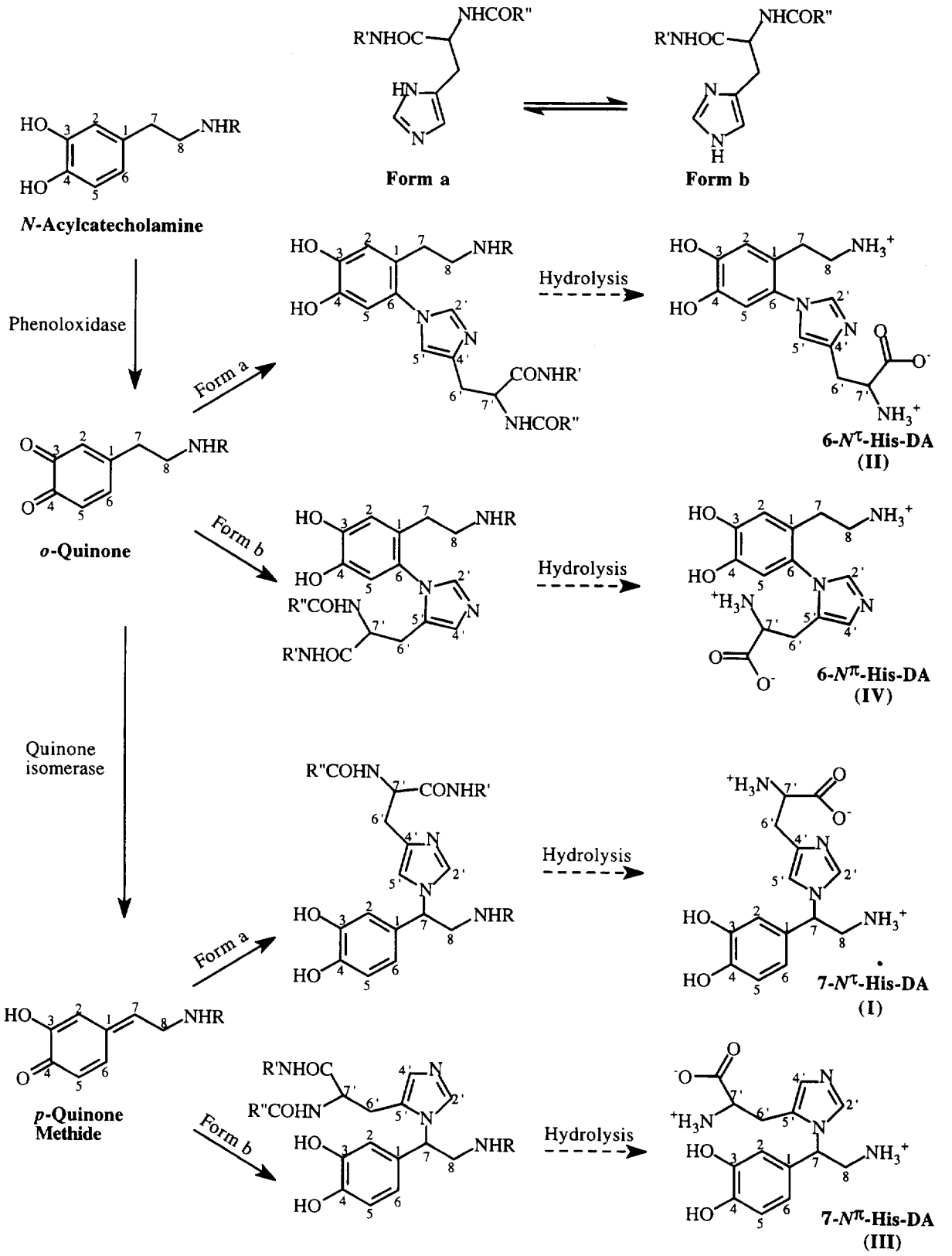

FIGURE 4. Proposed mechanism for *in vivo* protein-*N*-acylcatecholamine reactions in insect cuticle and their corresponding acid hydrolysis products. R=$-COCH_3$ or $-COCH_2CH_2NH_3+$, R′ and R″=polypeptide chains of protein. Note that dihedral angles C2–C1–C7–C8 (angle A) and C1–C7–N1′–C2′ (angle B) were used in the conformational searching for compounds I and III, and dihedral angles C2–C1–C7–C8 (angle C) and C1–C6–N′–C2′ (angle D) were used in the conformational searching for compounds II and IV.

hydrolysate in this study. The N^{τ}-adducts were present in the hydrolysate at approximately two-fold higher levels than the N^{π}-adducts. This result is consistent with the observation that a mixture of N^{τ} and N^{π} derivatives nearly always is produced during the direct ring alkylation of histidine, with the N^{τ} derivative most often the major product formed (Jain and Cohen, 1996).

Assuming that the adducts are quantitatively liberated from the cuticle and recovered from the acid hydrolysate, the molar ratio of the products suggests that 7-adducts are approximately twice as abundant as the 6-adducts. This result is not in agreement with solid-state NMR data indicating that C–N bonds made through catecholamine ring carbons are more abundant than C–N bonds made through side chain C7 (Schaefer *et al.*, 1987; Christensen *et al.*, 1991; Kramer *et al.*, 1995). Phenyl C2 and C5 also might be involved in C–N cross-links, which would enhance the C(ring)–N NMR signals, but we did not isolate any such adducts in the current study. Also, because the cuticle is not totally solubilized under our conditions, adduct liberation by acid hydrolysis may not be complete. Therefore, additional adducts might be present in the insoluble residue, as well as the unidentified catechol-containing products that we observed in the soluble fraction.

Based on these results, the following mechanism for the formation of protein–catecholamine adducts that give rise to the hydrolysis products characterized in this study can be rationalized (Fig. 4). The catecholamines first are oxidized to their *o*-quinones, which then are subjected to nucleophilic attack via a Michael 1,4-addition reaction by either of the imidazole nitrogens on histidyl residues in the cuticular proteins. Due to the facile mobility of the protons on nitrogens of the imidazole ring (Gilchrist, 1985), histidyl residues are present as tautomeric forms, giving rise to Form a and Form b in cuticular proteins. Nucleophilic additions of these histidyl residues to C6 of the *o*-quinones produce the 6-N^{τ}- and 6-N^{π}-adducts. Apparently, the *o*-quinones also are converted to *p*-quinone methides by a quinone isomerase (Sugumaran, 1988; Saul and Sugumaran, 1990; Hopkins and Kramer, 1992; Andersen *et al.*, 1996). Michael 1,6-additions of Form a and Form b to the *p*-quinone methides yield the 7-N^{τ}- and 7-N^{π}-adducts. In Fig. 4, the catecholamines are shown as free forms of NADA and NBAD, but they also might be bonded with other components to form catecholamine–chitin conjugates bonded through a phenoxy carbon–oxygen linkage or catecholamine–protein adducts of various structures (Okot-Kotber *et al.*, 1994, 1996).

These results provide for the first time actual structures of the cross-links that form from the reactions of quinonoid metabolites with proteins in insect cuticle undergoing sclerotization and underscore the important role of catecholamines as precursors for sclerotizing reagents. Our results are consistent with the hypothesis that quinones and quinone methides of *N*-acylcatecholamines, or NBAD in the case of *M. sexta* pupal cuticle, serve as cross-linking agents in insect cuticle by means of nucleophilic addition reactions with both of the imidazole nitrogens of histidyl residues of cuticular proteins. The structural identification of these His–DA adducts isolated from insect cuticle extends earlier results from solid-state NMR spectroscopic analyses, which first detected both ring and side chain catecholamine–histidine bonding (Schaefer *et al.*, 1987; Christensen *et al.*, 1991; Kramer *et al.*, 1995).

REFERENCES

Andersen S. O., Jacobsen J. P., Roepstorff P. and Peter M. G. (1991) Catecholamine–protein conjugates: isolation of an adduct of *N*-acetylhistidine to the side chain of *N*-acetyldopamine from an insect–enzyme catalyzed reaction. *Tetrahedron Lett.* **32,** 4287–4290.

Andersen S. O., Peter M. G. and Roepstorff P. (1992) Cuticle-catalyzed coupling between *N*-acetylhistidine and *N*-acetyldopamine. *Insect Biochem. Molec. Biol.* **22,** 459–469.

Andersen S. O., Peter M. G. and Roepstorff P. (1996) Cuticular sclerotization in insects. *Comp. Biochem. Physiol.* **113B,** 689–705.

Christensen A. M., Schaefer J., Kramer K. J., Morgan T. D. and Hopkins T. L. (1991) Detection of cross-links in insect cuticle by REDOR NMR spectroscopy. *J. Am. Chem. Soc.* **113,** 6799–6802.

Gilchrist T. L. (1985) *Heterocyclic Chemistry*, pp. 186–193. Pitman Publishing Ltd., Marshfield, MA.

Hopkins T. L., Morgan T. D. and Kramer K. J. (1984) Catecholamines in haemolymph and cuticle during larval, pupal and adult development of *Manduca sexta* (L.). *Insect Biochem.* **14,** 540–553.

Hopkins T. L. and Kramer K. J. (1992) Insect cuticle sclerotization. *Annu. Rev. Entomol.* **37,** 273–301.

Jain R. and Cohen L. A. (1996) Regiospecific alkylation of histidine and histamine at N-1 (*t*). *Tetrahedron* **52,** 5363–5370.

Kramer K. J., Hopkins T. L. and Schaefer J. (1995) Applications of solids NMR to the analysis of insect sclerotized structures. *Insect Biochem. Molec. Biol.* **25,** 1067–1080.

Matthews H. R. and Rapoport H. (1973) Differentiation of 1,4- and 1,5-disubstituted imidazoles. *J. Am. Chem. Soc.* **95,** 2297–2303.

Okot-Kotber B. M., Morgan T. D., Hopkins T. L. and Kramer K. J. (1994) Characterization of two high molecular weight catechol-containing glycoproteins from pharate pupal cuticle of the tobacco hornworm, *Manduca sexta*. *Insect Biochem. Molec. Biol.* **24,** 787–802.

Okot-Kotber B. M., Morgan T. D., Hopkins T. L. and Kramer K. J. (1996) Catecholamine-containing proteins from the pharate pupal cuticle of the tobacco hornworm, *Manduca sexta*. *Insect Biochem. Molec. Biol.* **26,** 475–484.

Pryor M. G. M. (1940) On the hardening of the cuticle of insects. *Proc. R. Soc. London Ser. B.* **128,** 393–407.

Pryor M. G. M. (1962) Sclerotization. In *Comparative Biochemistry, 4B* (Edited by Florkin M. and Mason H. S.), pp. 371–396. Academic Press, New York.

Saul S. J. and Sugumaran M. (1990) 4-Alkyl-*o*-quinone/2-hydroxy-*p*-quinone methide isomerase from the larval hemolymph of *Sarcophaga bullata*. I. Purification and characterization of enzyme-catalyzed reaction. *J. Biol. Chem.* **265,** 16992–16999.

Schaefer J., Kramer K. J., Garbow J. R., Jacob G. S., Stejskal E. O., Hopkins T. L. and Speirs R. D. (1987) Aromatic cross-links in insect cuticle: detection by solid-state ^{13}C and ^{15}N NMR. *Science* **235,** 1200–1204.

Sugumaran M. (1988) Molecular mechanisms for cuticular sclerotization. *Adv. Insect Physiol.* **21,** 179–231.

Sugumaran M. and Lipke H. (1982) Cross-link precursors for the dipteran puparium. *Proc. Natl. Acad. Sci. U.S.A.* **79,** 2480–2484.

Waite J. H. (1990) The phylogeny and chemical diversity of quinone-tanned glues and varnishes. *Comp. Biochem. Physiol.* **97B,** 19–29.

Xu R., Huang X., Morgan T. D., Prakash O., Kramer K. J. and Hawley M. D. (1996) Characterization of products from the reactions of

N-acetyldopamine quinone with *N*-acetylhistidine. *Arch. Biochem. Biophys.* **329,** 56–64.

Acknowledgements—We thank Dr Om Prakash [Kansas State University (KSU)] for conducting 2D NMR experiments, Gary Radke (KSU) for conducting MALDI–MS experiments, and Drs Dirk Friedrich (Hoechst Marion Roussel Inc.) and Christophe Morin (Université de Grenoble, France) for discussions about NMR experiments. We are also grateful to Leon Hendricks (Grain Marketing and Production Research Center) for providing *M. sexta* exuvial cuticle and Dr Svend O. Andersen (Copenhagen University) for a gift of the arterenone standard. We also thank Drs M. Dale Hawley (KSU), Jacob Schaefer (Washington University), Manickam Sugumaran (University of Massachusetts at Boston), Duy Hua (KSU), Om Prakash, Jianhua Liu (KSU), Dirk Friedrich, and Christophe Morin for critical comments about the manuscript. Research supported in part by National Science Foundation grant MCB-9418129. Cooperative investigation between the Kansas Agricultural Experiment Station (Contribution No. 97-57-J) and the U.S. Department of Agriculture. Mention of a proprietary product does not constitute a recommendation by the USDA. The Agricultural Research Service, USDA is an equal opportunity/affirmative action employer, and all agency services are available without discrimination.